

Article

Using Mixed Active Capping to Remediate Multiple Potential Toxic Metal Contaminated Sediment for Reducing Environmental Risk

Meng-Yuan Ou ¹, Yu Ting ¹, Boon-Lek Ch'ng ¹ , Chi Chen ¹, Yung-Hua Cheng ¹, Tien-Chin Chang ² and Hsing-Cheng Hsi ^{1,*} 

¹ Graduate Institute of Environmental Engineering, National Taiwan University, No. 1, Sec. 4, Roosevelt Rd., Taipei 10671, Taiwan; auanlie@outlook.com (M.-Y.O.); yuting821216@gmail.com (Y.T.); r06541135@ntu.edu.tw (B.-L.C.); q2461015@gmail.com (C.C.); r08541121@ntu.edu.tw (Y.-H.C.)

² Institute of Environmental Engineering and Management, National Taipei University of Technology, No. 1, Sec. 3, Zhongxiao E. Rd., Taipei 10608, Taiwan; tcchang@ntut.edu.tw

* Correspondence: hchsi@ntu.edu.tw; Tel.: +886-2-33664374

Received: 18 May 2020; Accepted: 27 June 2020; Published: 1 July 2020



Abstract: In this study, kaolinite, carbon black (CB), iron sulfide (FeS), hydroxyapatite (HAP), and oyster shell powder (OSP) were selected as potentially ideal amendments to immobilize metals in sediment, including Ni, Cr, Cu, Zn, and Hg. In aqueous batch experiments, the five adsorbents were tested for capturing the five potential toxic metals individually at various concentrations. HAP and OSP showed the largest removal efficiencies towards Ni (OSP: 76.47%), Cr (OSP: 100.00%), Cu (HAP: 98.39%), and Zn (HAP: 64.56%), with CB taking the third place. In contrast, FeS and CB played a more significant role in Hg removal (FeS: 100.00%; CB: 86.40%). In the modified six-column microcosm experiments, five mixing ratios based on various considerations using the five adsorbent materials were tested; the water samples were collected and analyzed every week for 135 days. Results showed that caps including CB could immobilize the release of Hg and methylmercury (MeHg) better than those with FeS. More economical caps, namely, with a higher portion of OSP in the mixed capping, could not reach comparable effects to those with more HAP for immobilizing Ni, but performed almost the same for the other four metals. All columns with active caps showed greater metal immobilization as compared to the controlled column without caps.

Keywords: active capping; toxic metal; sediment; remediation; multiple materials

1. Introduction

Wastewater containing potential toxic metals originating from anthropogenic activities discharged to river streams is a widespread environmental issue nowadays, processing significant toxicity to aquatic organisms and accumulating by food chain, finally causing various diseases and disorders [1]. Natural processes are frequently inadequate to deal with the elevated metal loading, therefore there is an urgent need for remediation measures [2]. Thin-layer capping has been applied as an economically-feasible in-situ method for sediment remediation, reducing contaminants release from sediment to overlying water, subsequently reducing ecological and human health risk [3]. Sediment can be seen as an important sink of various organic and inorganic compounds, resulting in the simultaneous existence of several different contaminants [4–6]. However, most of the previous studies focused on only one or two capping materials. To cope with highly complex conditions in sediment, mixed capping with multiple materials was proposed. Notably, using cheap and effective alternatives for the removal of potential toxic metals could reduce operating costs, reduce the prices of products, improve competitiveness, and benefit the environment [7].

Several relatively cheap, environment-friendly materials have been proposed and examined. Based on previous research [7–22], kaolinite, carbon black (CB), iron sulfide (FeS), oyster shell powder (OSP), and hydroxyapatite (HAP; $\text{Ca}_{10}(\text{PO}_4)_6(\text{OH})_2$) were considered as potentially ideal amendments to be part of the mixed caps. Previous reports provided excellent results showing that kaolinite can be used as a cheap and naturally occurring adsorbent to remove Pb^{2+} , Cd^{2+} , Ni^{2+} , Co^{2+} , Cr^{6+} , Zn^{2+} , and Cu^{2+} from aqueous solution in both single and multi-metal ions [8–11]. Sulfide minerals are shown to be ideal materials to scavenge Hg^{2+} by immobilizing it through adsorption or co-precipitation as a discrete sulfide phase (HgS) and solid solution formation with iron sulfides [12,13]. HAP jumped out recently because of its high adsorption capacity of various metals, which brings the perspective for removal of Cd^{2+} , Zn^{2+} , Pb^{2+} , U^{6+} , Co^{2+} ions, and so on [14–17]. HAP is a nanostructured material, which was recently synthesized from some high-calcium biological wastes as raw materials, such as seashells and eggshells [18]. In the hunt of such low-cost and efficient raw materials for the production of HAP, OSP has emerged as a suitable one. As for OSP itself, owing to its low price and basicity, it has been employed widely for stabilization/solidification of many kinds of potential toxic metals (As, Pb, Ni, and Cu, etc.) [7,19–22]. The solution pH of OSP greatly affected the adsorption process towards Cu^{2+} , with an optimum adsorption pH of 5.5 and an overall negative surface charge facilitating the adsorption process [19]. The adsorption capacities of OSP towards Cu^{2+} and Ni^{2+} could reach $49.26\text{--}103.1\text{ mg g}^{-1}$ and $48.75\text{--}94.3\text{ mg g}^{-1}$, respectively, through physical adsorption mechanisms [7].

The present study aims to find mixed amendments with the best comprehensive benefits for immobilizing potential toxic metals in contaminated sediment. Based on the previous works, kaolinite, CB, FeS, OSP, and HAP were selected as potentially ideal amendments to immobilize metals in sediment. According to the survey report of Taiwan in 2012 [23] on main rivers with contaminated sediment, Ni, Cr, Cu, Zn, and Hg are the five major potential toxic metals present in sediments, which were selected as the targets of remediation in this study. Furthermore, methylmercury (MeHg) converted from Hg was measured in this study due to its high toxicity and bioaccumulative ability. Aqueous batch experiments were first conducted by using the five adsorbents to capture the five potential toxic metals individually at various concentrations. Then, five columns containing contaminated sediment covered by different mixed materials were set based on the obtained results of batch experiments to better comprehend the immobilization effectiveness of mixed capping for the potential toxic metals as compared to the controlled column without caps. Results from this study are helpful in designing an economically and technically feasible in-situ approach for sediment remediation, which could not only reduce the potential toxic metal release from sediment to overlying water, but also reduce the ecological and human health risk.

2. Materials and Methods

2.1. Adsorbents Preparation

The kaolinite and FeS used in this study were all reagent-grade chemicals purchased from Sigma-Aldrich. The CB used was obtained from Enrestec Inc. (Tainan, Taiwan), and was considered as a low-cost, recycled materials because it was a byproduct from waste rubber tire pyrolysis for oil production.

OSP was prepared by grinding oyster shells collected as food waste materials. The oyster shells were scrubbed carefully to remove impurities, then dried for 48 h at $100\text{ }^\circ\text{C}$ [19] and ground to homogenized powder that could pass through a 30-mesh sieve. Then this sieved material was shaken over a 60-mesh sieve and any material that passed through was rejected (ASTM D2765). [24]

To synthesize HAP, the OSP passed through the 60-mesh sieve was collected as a raw material. The synthesis was operated according to the following reaction: $10\text{Ca}^{2+} + 6\text{PO}_4^{3-} + 2\text{OH}^- = \text{Ca}_{10}(\text{PO}_4)_6(\text{OH})_2$, referring to previous studies [18,25–27] (Figure 1). In the synthesis process, an amount of Na_2HPO_4 and the corresponding amount of oyster shell powder (Ca/P molar ratio = 1.67) were used as P and Ca precursors, respectively. Firstly, 5 g of that oyster shell powder (<60 mesh) was dissolved

in 1:3 hydrochloride acid/water solution and stirred thoroughly. The supernatant of the solution filtered by $0.45\ \mu\text{m}$ filter was put into 500 mL of 0.1 M EDTA. Then reaction process was carried out by drop wise addition of 0.06 M Na_2HPO_4 solution under continuous stirring of 200 rpm. The pH value of the reaction mixture was regulated within the range of 10.5–11.5 by 5 M NaOH solution and maintained throughout the process the dripping velocity was controlled at $2\ \text{mL min}^{-1}$. After mixing, the resulting mixture was left to mature for the next 24 h. The obtained white precipitate was washed with distilled water by centrifuge and dried in the hot air oven at $65\ ^\circ\text{C}$ for 24 h to get the final product.

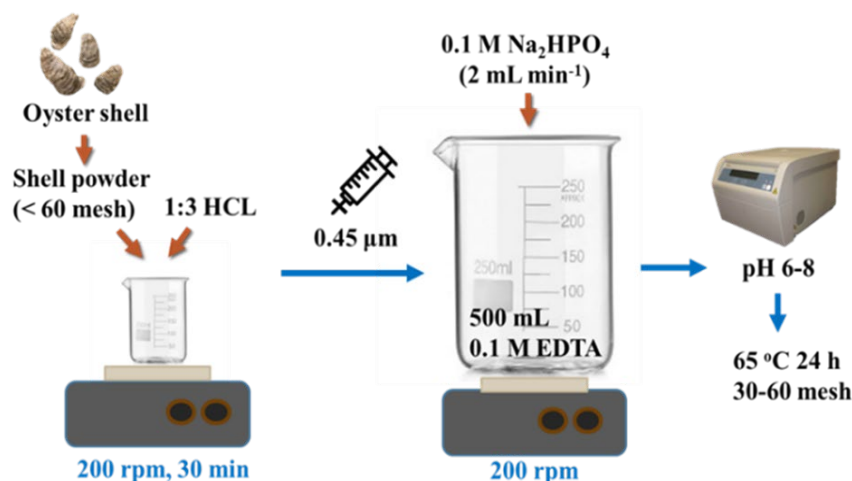


Figure 1. The process of synthesizing HAP.

All of the above materials were sieved to the range of 30–60 mesh (ASTM D2765) [24] and analyzed using a physisorption analyzer (Micromeritics Inc. ASAP 2420, Norcross, GA, USA) to obtain the 77 K N_2 adsorption isotherm. The total surface area was then obtained based on the Brunauer-Emmett-Teller (BET) equation and described as BET surface area (S_{BET}). The chemical compositions of the five materials were analyzed for the C/H/N/S contents (Elementar Vario EL cube, Langensfeld, Germany) and O content by automatic elemental analyzers (Flash 2000, Thermo Fisher Scientific, Waltham, MA, USA).

2.2. Artificial Fresh Water and Sediment Incubation

In order to simulate the river environment, artificial freshwater prepared based on the formula provided by USEPA [28] was used in this system, instead of using purified or deionized water. To prepare 20 L of synthetic, moderately hard, reconstituted fresh water, the reagent grade chemicals as follows were used: 1.20 g MgSO_4 , 1.92 g NaHCO_3 , 0.080 g KCl, and 1.06 g CaSO_4 .

The metal incubation concentrations of artificial sediment and reagent grade chemicals were determined with reference to the survey report of Taiwan in 2012 [23] on main rivers with contaminated sediment. The sediment was designed to consist of $400\ \text{mg kg}^{-1}$ Ni, $400\ \text{mg kg}^{-1}$ Cr, $1000\ \text{mg kg}^{-1}$ Cu, $1000\ \text{mg kg}^{-1}$ Zn, and $50\ \text{mg kg}^{-1}$ Hg by adding $\text{Ni}(\text{NO}_3)_2 \cdot 6\text{H}_2\text{O}$, $\text{Cr}(\text{NO}_3)_3 \cdot 9\text{H}_2\text{O}$, $\text{Cu}(\text{NO}_3)_2 \cdot 3\text{H}_2\text{O}$, $\text{Zn}(\text{NO}_3)_2 \cdot 6\text{H}_2\text{O}$, and HgCl_2 . The sediment (2000 g) was placed in a 3 L glass bottle, filled with artificial freshwater, mixed thoroughly, sealed tightly, and put aside for incubation. The time of incubation lasted up to 60 days.

2.3. Aqueous Batch Experiments

The aqueous adsorption experiment was performed according to Bouhamed et al. [1]. To determine the adsorption isotherms of adsorbents, 10, 30, and $50\ \text{mg L}^{-1}$ of Ni, Cr, Cu, and Zn were tested by aqueous batch experiments. For Hg, 0.2, 0.6, and $1.0\ \text{mg L}^{-1}$ were tested. A serial dilution of standard solution was made to the intended concentrations; the pH value of the solution was

controlled to be 5 ± 0.1 by using 0.01 M NaOH and 0.01 M HCl, which simulates the real contaminated sediment environment.

Batch adsorption experiments were carried out in a rotary shaker at 125 rpm using 50 mL capped glass bottles containing 20 mL of metal ion solutions and 25 mg of adsorbents, similar to our previous study [29]. The temperature was controlled at 30 °C and the contact time was up to 24 h to achieve an adsorption equilibrium. All the experimental operations were triplicated.

After shaking, samples were filtered with 0.45 μm filters and the supernatant was kept for metal analyses. For a long-time preservation, each sample of Ni, Cr, Cu, and Zn was preserved with 0.5% HNO_3 and measured by flame atomic absorption spectroscopy (FAAS; Perkin Elmer AAnalyst 800, Waltham, MA, USA); each sample of Hg was preserved with 0.5% BrCl and estimated by cold vapor atomic fluorescence spectroscopy (CVAFS; Brooks Rand Automated Total Mercury System, Seattle, WA, USA). QA/QC were regularly checked by analyzing duplicate samples and quality control samples from each batch.

2.4. Microcosm Experiments

2.4.1. Microcosm Design

The microcosm shown in Figure 2 was designed by modifying the system used in Ting et al. [29]. Multi-columns containing contaminated sediment with mixed caps on the top were set to stimulate the release of metal compounds and examine the efficiencies of capping materials. Water entered the system from the bottom of the column, vertically moved upwards to fill the column, and then discharged to the outside of the system.

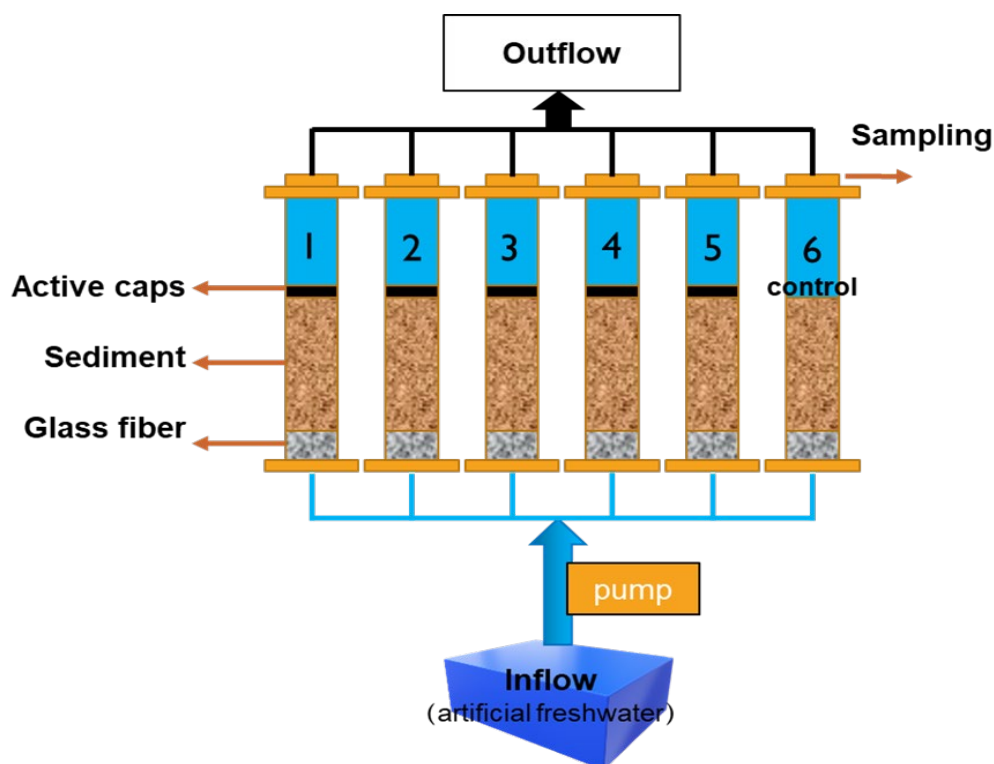


Figure 2. The lab-scale microcosm system.

2.4.2. Microcosm Operation

Six freshwater columns were set up to investigate the efficiencies and stabilities of different mixed caps. Dried incubated sediment was added into the columns and each column contained 200 g of sediment. Five columns were capped by the mixed adsorbents with five different ratios, which were

determined according to the results of batch experiments. The sixth column was not capped as the controlled unit. To start up the system, each column was filled with water and allowed to settle for 24 h. Next, the microcosm was activated to start inflow and this day was counted as the operation day 1. The flow rate was maintained to be 0.2 L day⁻¹ constantly by using a peristaltic pump (Gamma ST100SV2, Shakopee, MN, USA).

Notably, in order to investigate the stabilization of different mixed caps, the pH of artificial water was adjusted to 3 ± 0.1 by adding HNO₃ during day 101–114 to simulate the extreme condition with acid influent.

2.4.3. Water Sampling and Analyses

Periodic water sampling was conducted continuously once a week for up to two months. At each sampling time, the pH, dissolved oxygen (DO), electrical conductivity (EC), oxidation-reduction potential (ORP) were measured one by one initially. DO of the overlying water was directly measured by a DO meter (EXStik DO600, Nashua, NH, USA). pH value was measured by a pH meter (SunTex SR-2300, Hsi-Chih, Taipei, Taiwan). The electrical conductivity (EC) was measured by a conductivity meter (Taina EZDO-6021, Taiwan). The oxidation–reduction potential (ORP) of sediment within the depth of 1–3 cm of caps was measured by an ORP meter (SunTex SR-2300, Hsi-Chih, Taipei, Taiwan). After the basic measurement, 100 mL of water was collected from each column by disposable syringes and filtered with 0.45 µm filter membranes. The supernatant was kept in 20 mL glass bottles in a refrigerator at 4 °C before analyses.

The samples prepared for Hg analysis were preserved with 0.5% BrCl. For Ni, Cr, Cu, and Zn analyses, samples were preserved with 0.5% HNO₃ and determined by inductively coupled plasma optical emission spectrometry (Agilent ICP-OES 700 series, Santa Clara, CA, USA). For MeHg analysis, samples were put in brown bottles in the shadows to avoid light and analyzed immediately by ethylation, purge and trap, and gas chromatography/CVAFS (Brooks Rand Automated Total Mercury System, Seattle, WA, USA). Total organic carbon (TOC) was analyzed by a TOC analyzer (OI Analytical Aurora 1030W, College Station, TX, USA). QA/QC were regularly checked by analyzing the quality control samples from each batch.

2.4.4. Statistical Analysis

A one-way ANOVA, followed by a least significant difference (LSD) test ($p < 0.05$), was used to determine the significance differences among columns (IBM SPSS statistics).

3. Results

3.1. Adsorbents Properties

Five capping adsorbents, sieved to 30–60 mesh, were analyzed and their physical and chemical properties are summarized in Table 1, including the BET surface areas (S_{BET}), average pore sizes, and total pore volumes (V_{total}). The data revealed that HAP had the absolutely largest BET surface area and pore volume among these five materials, and CB had a relatively larger specific surface area and the second largest pore volume.

Table 1. BET surface areas, average pore sizes and total pore volumes (V_{total}) of five materials.

Adsorbent	S_{BET} (m ² g ⁻¹)	Pore Size (nm)	V_{total} (cm ³ g ⁻¹)
Kaolinite	23.3	14.0	0.082
FeS	106.2	60.2	0.042
CB	93.0	17.3	0.376
HAP	367.4	9.2	0.501
OSP	0.06	4.8	0.011

The results of element analyses of the five materials are given in Table 2. FeS was not analyzed and theoretically it is composed of 63.64 wt% of iron and 36.36 wt% of sulfur. It can be seen that CB was rich in C (77.87 wt%) and had a great amount of S (2.53 wt%) because it originated from waste tire. OSP and HAP were rich in O (32.29 and 13.24 wt%, respectively). The proportions of C in OSP roughly corresponded to the proportion of CaCO₃ in oyster shell.

Table 2. Elemental analyses of the five test materials.

Adsorbent	C (wt%)	N (wt%)	H (wt%)	O (wt%)	S (wt%)
Kaolinite	0.03	0.15	1.43	10.88	0.05
FeS			-		
CB	77.87	0.46	1.02	1.6	2.53
HAP	0.00	0.11	1.71	13.24	0.00
OSP	11.61	0.20	0.55	32.29	0.07

3.2. Adsorption Efficiency

The aqueous metal removal efficiency by the adsorbents was calculated with the following equation:

$$R = \frac{C_0 - C_t}{C_0} \times 100\%, \quad (1)$$

where R (%) is the removal efficiency of adsorbents, C₀ (mg L⁻¹) is the initial metal concentration detected in blank solution, and C_t (mg L⁻¹) is the concentration of remaining sorbate at any time.

Figure 3 and Table 3 show the removal efficiencies of five materials towards five metals at various initial concentrations, which illustrated roughly that OSP and HAP had the best affinities to Cr, Zn, Cu, and Ni, and CB took the third place. As for Cu, HAP performed the largest removal efficiency than the others with a reduction of 98.39%. For Ni, OSP presented a significant removal rate of 76.47% at a low initial concentration and, contrarily, poor efficiency at high initial metal concentrations. For the adsorption of Hg, inversely, FeS showed the best removal efficiency, which was up to 100%. CB was the second excellent one with a removal rate of 86.4%.

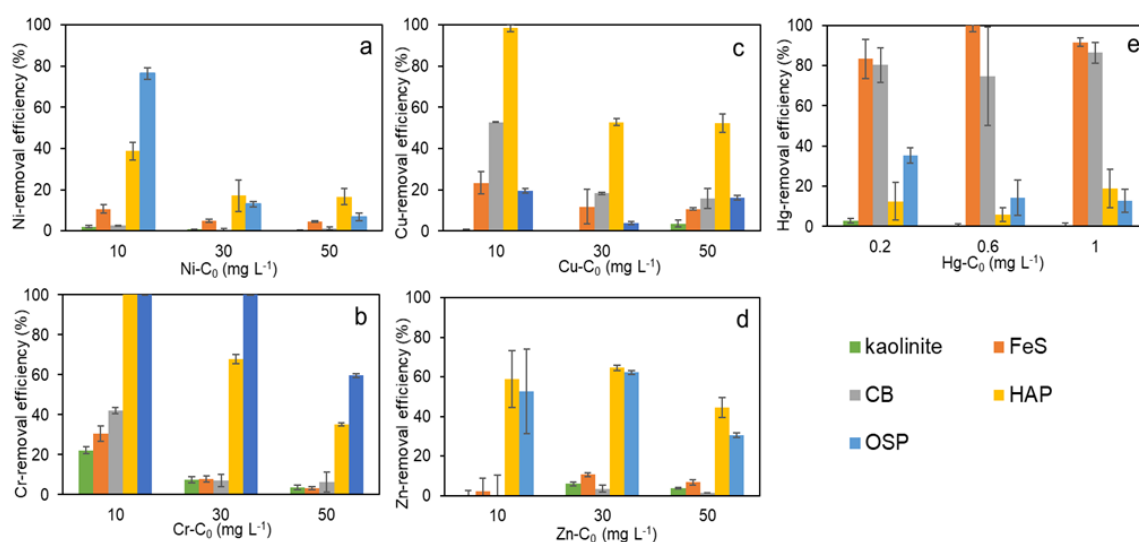


Figure 3. Removal efficiencies of five materials towards (a) Ni, (b) Cr, (c) Cu, (d) Zn, and (e) Hg at various initial concentrations.

Table 3. Removal efficiencies (in percentage) of five adsorbents for five metals ($n = 3$).

Metal	C_0 (mg L ⁻¹)	Kaolinite	FeS	CB	HAP	OSP
Ni	10	2.04 ± 0.50	10.73 ± 1.98	2.60 ± 0.27	38.85 ± 4.36	76.47 ± 2.73
	30	0.86 ± 0.12	4.96 ± 0.91	0.60 ± 0.53	17.11 ± 7.56	12.99 ± 1.19
	50	0.41 ± 0.15	4.63 ± 0.48	1.37 ± 0.72	16.62 ± 3.98	6.85 ± 1.81
Cr	10	22.15 ± 1.66	30.65 ± 3.85	42.00 ± 1.41	102.58 ± 0.15	103.13 ± 0.03
	30	7.38 ± 1.61	7.88 ± 1.63	6.98 ± 3.11	67.81 ± 2.30	105.18 ± 0.07
	50	3.73 ± 1.10	3.07 ± 0.77	6.19 ± 5.09	35.06 ± 0.73	59.58 ± 0.90
Cu	10	-1.13 ± 0.95	23.45 ± 5.41	52.80 ± 0.21	98.39 ± 1.65	19.43 ± 1.17
	30	-0.20 ± 0.11	11.89 ± 8.29	18.27 ± 0.41	52.90 ± 1.85	3.82 ± 0.76
	50	3.69 ± 1.83	10.78 ± 0.69	15.91 ± 4.83	52.41 ± 4.46	16.05 ± 1.14
Zn	10	-6.63 ± 2.65	2.09 ± 6.73	-29.32 ± 10.30	58.88 ± 14.26	52.71 ± 21.53
	30	5.86 ± 0.81	10.55 ± 1.03	3.47 ± 1.62	64.56 ± 1.20	62.30 ± 0.98
	50	3.69 ± 0.45	6.71 ± 1.33	1.44 ± 0.00	44.38 ± 5.02	30.62 ± 1.21
Hg	0.2	2.93 ± 1.23	83.37 ± 9.65	80.30 ± 8.55	12.48 ± 9.35	35.32 ± 3.81
	0.6	-2.36 ± 1.15	101.12 ± 3.15	74.70 ± 24.47	5.92 ± 3.47	14.43 ± 8.85
	1	-0.50 ± 1.75	91.51 ± 2.10	86.40 ± 5.09	18.86 ± 9.43	12.86 ± 5.70

3.3. Microcosm

3.3.1. Mixed Caps Design

Five columns covered by different mixed materials and one controlled column were set as shown in Table 4 for conducting the microcosm experiments. The design of capping mixing ratio was based on the integrating consideration of removal efficiencies, cost of preparation, and utilization of recycling resources.

Table 4. Six columns covered by different mixed materials.

Column	1	2	3	4	5	6
kaolinite (wt%)	10	10	10	10	-	
FeS (wt%)	2.5	-	5	2.5	2.5	
CB (wt%)	2.5	5	-	2.5	2.5	
HAP (wt%)	35	35	35	5	35	
OSP (wt%)	50	50	50	80	50	
Total (wt%)	100	100	100	100	90	

Based on the aforementioned results from batch experiments, HAP and OSP were selected as the major materials to adsorb Ni, Cr, Cu, and Zn; FeS and CB were selected as the major materials to immobilize total Hg (THg) and MeHg. Although the adsorption effect of kaolinite on these five metals was not significant, it has been shifted that kaolinite may probably be more capable of stabilizing the caps than other clays [30] and was therefore added for the purpose of resisting flow disturbance. Column 1 was designed as the ideally best column with appropriate amounts of each material. Column 2 replaced FeS completely with CB and Column 3 did the opposite for comparing FeS with CB. As far as costs and complexity of preparation were concerned, Column 4 tried to reduce the proportion of HAP to grope for a cheaper mixed amendment with equal ability. The cap ratio of Column 5 was almost the same as Column 1, except for the absence of 10 wt% kaolinite, which was designed to investigate the necessity of existence of kaolinite. The last column was composed of only sediment without caps as the controlled group.

3.3.2. Results of Sediment Incubation

The concentrations of the five metals before and after 60 days of incubation and the concentrations of the five metals in the supernatant after incubation are shown in Table 5. Concentrations of metals in the sediment after incubation had almost met the experimental requirements. It is worth mentioning

that the concentrations of Ni and Zn of supernatant were much higher than those of the other three metals.

Table 5. Concentrations of the five metals in sediment before and after 60 days of incubation and the concentrations of the five metals in the supernatant after incubation.

Metal	Sediment (mg kg ⁻¹)			Supernatant (mg L ⁻¹)
	Before	Design	After	
Ni	61.35 ± 1.46	400	519.59 ± 9.52	133.46 ± 0.98
Cr	102.16 ± 0.63	400	593.96 ± 2.81	0.16 ± 0.002
Cu	94.64 ± 2.38	1000	1383.30 ± 6.58	17.71 ± 0.12
Zn	373.70 ± 12.18	1000	1579.13 ± 14.31	358.79 ± 1.06
THg	0.20 ± 0.03	50	72.32 ± 1.96	0.03 ± 0.008
MeHg	$1.50 \times 10^{-4} \pm 2.54 \times 10^{-5}$	–	$8.56 \times 10^{-3} \pm 3.23 \times 10^{-3}$	–

3.3.3. pH and ORP

Figure 4 shows the changes of oxidation-reduction potential (ORP) and water pH in the microcosm during the operation. The data of changes of electrical conductivity (EC), pH, dissolved oxygen (DO), and oxidation-reduction potential (ORP) are also shown in Tables S1–S4. Higher pH values and lower ORP in columns capped with materials were attained as compared to the one without caps. However, the differences tended to be slight during the later stage.

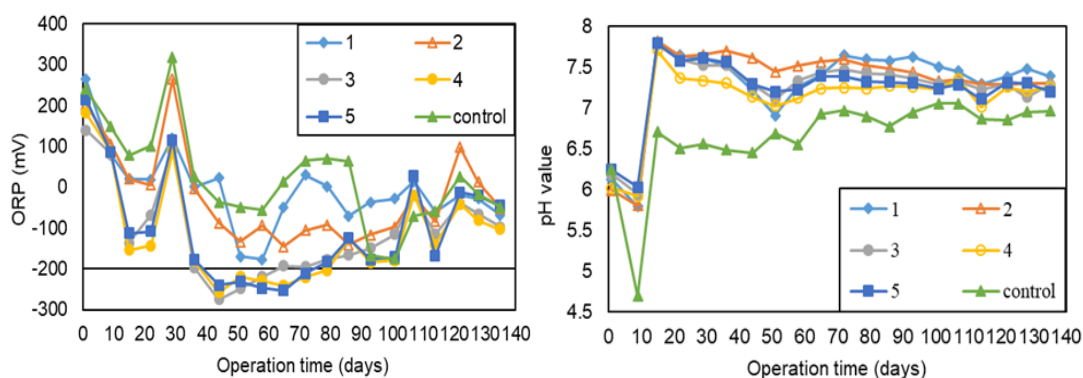


Figure 4. The changes of oxidation-reduction potential (ORP) and water pH values in microcosm during the operation.

3.3.4. Metal Immobilization

The concentrations of five metals and MeHg are shown in Figure 5 and Tables S5–S10 (in Supplementary Material). The results of one-way ANOVA and LSD test ($p < 0.05$) are shown in Tables 6 and 7. In consistence with the expectation, Column 1 showed the most considerable comprehensive consequences of inhibiting the release of metals to the overlying water. It was unexpected that even without 10 wt% of kaolinite, Column 5 achieved almost the same results as Column 1, which is also proved by no significant ($p > 0.05$) correlation in ANOVA (Table 6) between the two columns for all metals, indicating that kaolinite did not show greater stabilization ability for mixed caps as compared to the other test materials.

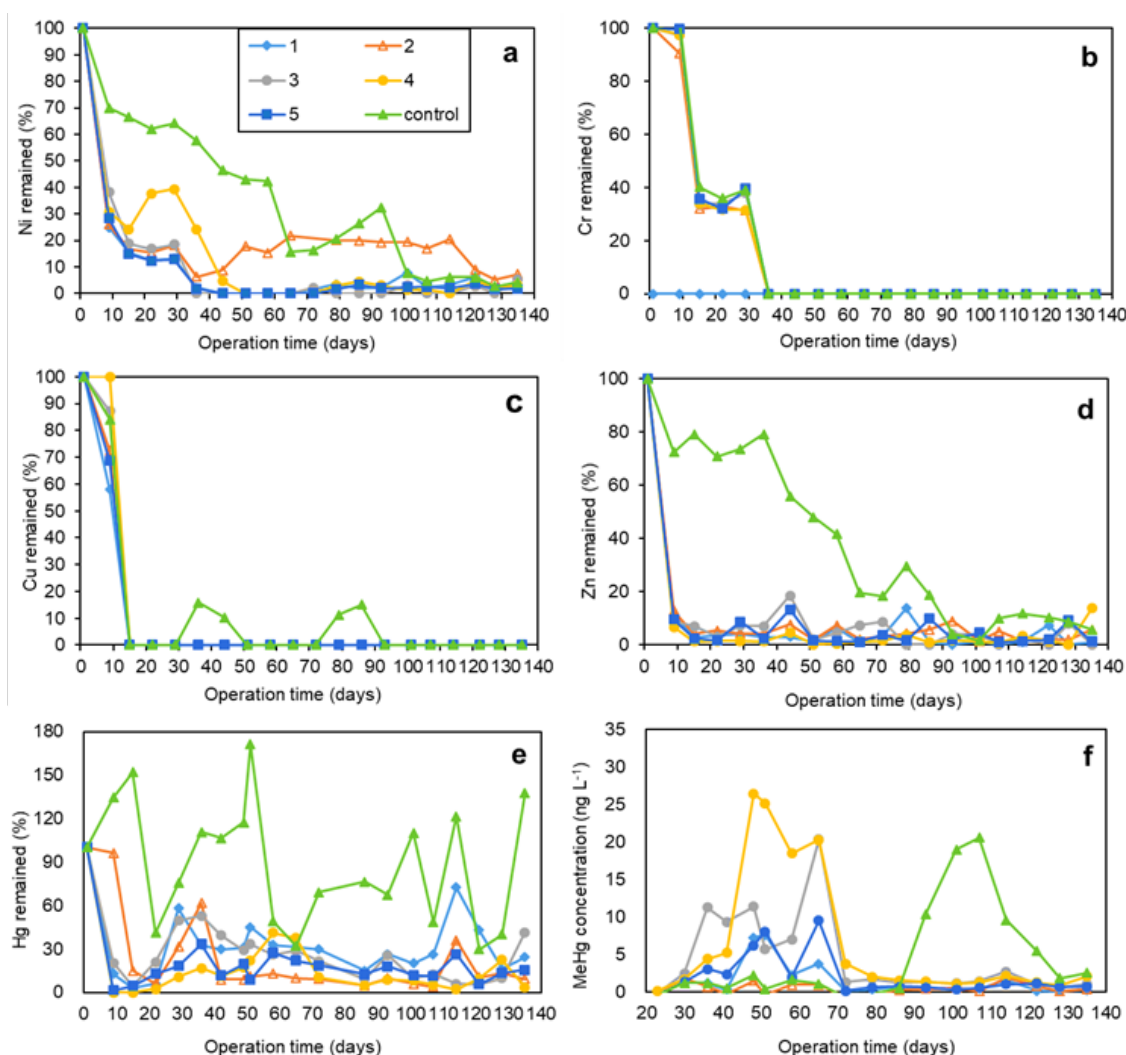


Figure 5. The remaining proportion (%) of (a) Ni, (b) Cr, (c) Cu, (d) Zn, (e) Hg, and (f) the concentration of MeHg in six columns. The remaining proportion in aqueous phase was calculated through dividing the concentration of each contaminant by the concentration on the first day.

Table 6. Metal concentrations in six columns before adding acid (day 1–100).

Column	Ni (<i>n</i> = 14) (mg L ⁻¹)	Cr (<i>n</i> = 14) (mg L ⁻¹)	Cu (<i>n</i> = 14) (mg L ⁻¹)	Zn (<i>n</i> = 14) (mg L ⁻¹)	THg (<i>n</i> = 14) (μg L ⁻¹)	MeHg (<i>n</i> = 12) (ng L ⁻¹)
1	0.091 ± 0.189 ^b	0.000 ± 0.000 ^a	0.013 ± 0.036 ^a	0.150 ± 0.354 ^b	0.145 ± 0.109 ^c	2.09 ± 2.68 ^{bc}
2	0.162 ± 0.157 ^b	0.015 ± 0.025 ^a	0.012 ± 0.030 ^a	0.140 ± 0.289 ^b	0.382 ± 0.463 ^{ab}	0.535 ± 0.622 ^c
3	0.064 ± 0.126 ^b	0.015 ± 0.025 ^a	0.010 ± 0.027 ^a	0.090 ± 0.182 ^b	0.233 ± 0.166 ^{bc}	6.06 ± 6.09 ^{ab}
4	0.140 ± 0.200 ^b	0.016 ± 0.026 ^a	0.012 ± 0.031 ^a	0.131 ± 0.385 ^b	0.288 ± 0.373 ^{abc}	9.18 ± 10.2 ^a
5	0.079 ± 0.165 ^b	0.015 ± 0.025 ^a	0.012 ± 0.031 ^a	0.135 ± 0.311 ^b	0.178 ± 0.194 ^{bc}	2.85 ± 3.25 ^{bc}
6	0.315 ± 0.161 ^a	0.015 ± 0.025 ^a	0.018 ± 0.035 ^a	0.498 ± 0.288 ^a	0.496 ± 0.222 ^a	1.56 ± 2.85 ^c

Different letters for metal concentrations in six columns indicate a significant difference at *p* < 0.05. For example, the concentrations of Ni in Column 1 with letter b are significantly different from the concentrations of Ni in Column 6 with letter a.

When comparing Column 1 (50% OSP + 35% HAP) with Column 4 (80% OSP + 5% HAP), it is demonstrated by Figure 5 that the releases of Ni, Cr, Cu, and Zn were inhibited well in both columns. However, Column 4 with less proportion of HAP could not achieve an equal effect to Column 1 for Ni, Cr and MeHg immobilization (Figure 5), and a significant correlation was observed by ANOVA (*p* < 0.05) (Table 6) in MeHg concentrations of the two columns (Table 6).

Table 7. Metal concentrations in six columns after adding acid (day 101–135)

Column	Ni ($n = 6$) (mg L ⁻¹)	Zn ($n = 6$) (mg L ⁻¹)	THg ($n = 6$) (μg L ⁻¹)	MeHg ($n = 6$) (ng L ⁻¹)
1	0.029 ± 0.017 ^{ab}	0.024 ± 0.038 ^b	0.151 ± 0.094 ^b	0.453 ± 0.544 ^b
2	0.029 ± 0.017 ^{ab}	0.033 ± 0.022 ^{ab}	0.182 ± 0.162 ^b	0.605 ± 0.672 ^b
3	0.009 ± 0.010 ^c	0.017 ± 0.023 ^b	0.100 ± 0.096 ^b	1.29 ± 0.729 ^b
4	0.016 ± 0.012 ^{bc}	0.049 ± 0.076 ^{ab}	0.121 ± 0.106 ^b	1.42 ± 0.532 ^b
5	0.015 ± 0.005 ^{bc}	0.038 ± 0.039 ^{ab}	0.113 ± 0.057 ^b	0.721 ± 0.311 ^b
6	0.035 ± 0.011 ^a	0.078 ± 0.036 ^a	0.433 ± 0.251 ^a	9.80 ± 8.20 ^a

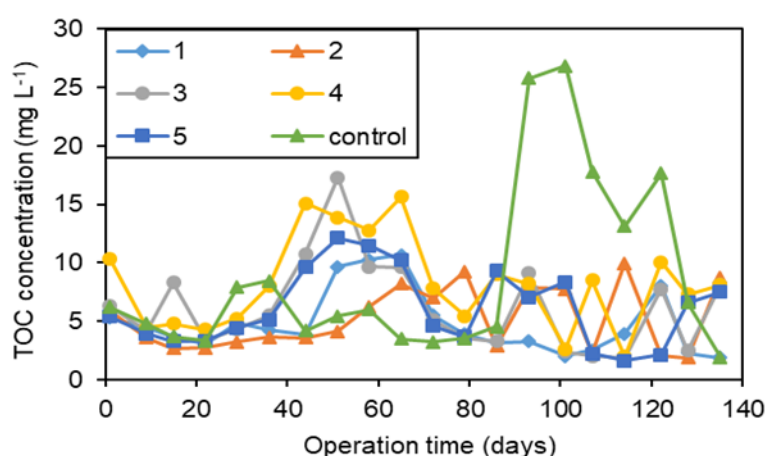
Different letters for metal concentrations in six columns indicate a significant difference at $p < 0.05$. For example, the concentrations of Ni in Column 1 with letter a and b are significantly different from the concentrations of Ni in Column 3 with letter c.

To compare FeS with CB, 5% FeS in Column 3 made it more effective in immobilizing Ni than 5% CB in Column 2. On the other hand, Column 3 did worse than Column 2 for lowering the concentration of MeHg in the long term, which was demonstrated doubly by Figure 5 and statistical analysis (Table 6).

The stabilization of different mixed caps under extreme condition with acid influent during day 101–114 is also shown in Figure 5. It was observed that the concentrations of Hg and MeHg in every column increased during the days with acid influent (Figure 5f), especially for the controlled column without capping (Table 7). Also, Column 6 released the most amount of Zn during day 101–114 (Figure 5d). The experimental results also suggested that columns with caps were less affected by acid influent than the controlled one, which could be supported by strong significant correlations observed by ANOVA between Column 6 and the other columns.

3.3.5. Total Organic Matter (TOC)

Figure 6 shows that the amount of TOC was positively related to the concentration of MeHg. Column 4, with the largest percentage of OSP, released maximum MeHg during day 20–80. In a later stage from approximately day 85, however, both MeHg and TOC concentrations in Column 6 increased suddenly.

**Figure 6.** Total organic carbon (TOC) in six columns during the operation

4. Discussion

The data of material properties showed the absolutely largest BET surface area and pore volume of HAP, CB, and FeS, which may lead to its excellent performance during adsorption due to more adsorption sites. In contrast, OSP is a non-porous material with insignificant surface area and pore volume, but OSP still had appreciable adsorption performance for several metals, suggesting that the adsorption behavior of OSP is different with its derived HAP. Abundant C content in CB indicated its

additional benefits as an active material [31]. HAP was rich in H and O, probably as a result of the richness of hydroxyl groups on its surface [32], contributing to its high ability as a metal scavenger [33].

In the part of batch experiments, OSP and HAP had the optimum removal efficiencies for Cr, Zn, Cu, and Ni. HAP is regarded as an ideal material with large specific surface and high stability under both reducing and oxidizing conditions [16]. It can release phosphate to interact with metals, forming metal phosphates of low water solubility [34]. OSP has been proven to be able to raise the pH value when applied to soil [35]. If the pH is above the value that promotes metal precipitation, the removal mechanisms will be related to precipitation [36]. However, it is known that the hydroxides of Ni have the highest solubility product (K_{sp}) among those of the five metals, making it comparatively difficult for Ni to be removed by precipitation. As for Hg, FeS and CB showed the best immobilizing ability due to their high Hg affinity. Notably, the CB used in this study was a waste tire recycled product, which contains a significant amount of S that can form chemical bonding with Hg.

The metal potential leachability could determine their environmental risks, and it has been reported to decrease in the order of Zn > Ni > Cu > Cr at pH 4 [37], which corresponded to the concentrations of the five metals in the supernatant after incubation, revealed stronger leachability of Ni and Zn, and was related to their behaviors in the microcosm.

It is generally accepted that sediment pH is an important factor in the adsorption of adsorbate on adsorbent. Under low pH condition, most metal ions are in the cationic state in the solution. The hydrogen ions can compete for the adsorption sites with the metal ions, influencing the exchange adsorption of potential toxic metals, promoting the desorption of metal ions and causing a higher release rate [38,39]. The ability of OSP to raise the concentration of hydroxide ions mentioned before may account for the increase of pH in the columns and its high removal capacity of metals. As one of the most important factors influencing the mobility of metals, the increase of ORP in sediment will correspondingly promote the oxidization of metal sulfides and the degradation of organic compounds, both accelerating the release of the adsorbed/complexing metals [40]. It appeared that ORP of Column 6 was higher than the other five capped in general, mainly due to the decrease of dissolved oxygen caused by caps in the other five columns.

In the part of the lab-scale microcosm experiments, the data from Column 5 indicated the unnecessary existence of kaolinite whether for adsorption or for stabilization in such a condition, which is inconsistent with the suggestions from some earlier studies. The reason may be due to that HAP and OSP could play the same role as kaolinite to stabilize the caps. The difference between Column 1 and Column 4 shown in Figure 5 was related to different performances of HAP and OSP to remove Ni as Figure 3a illustrated. Nevertheless, using caps mainly composed of OSP can yet be regarded as a good choice when considering costs. In batch adsorption, FeS showed the third best adsorption ability for Ni by a reduction of 10.73%, and yet CB hardly worked (Figure 3a). Thus, the release in the later stage of the experiment of Ni in Column 2 may be due to the ineffectiveness of CB. In contrast, Column 3 (5% FeS) did worse than Column 2 (5% CB) for lowering the concentration of MeHg in the long term (Figure 3f). FeS can reduce the concentration of soluble Hg species, resulting in less methylation of Hg [41]. Moreover, part of FeS was likely to be converted into insoluble HgS and taken out by the overlying water, which may explain the unsuccessful results of Column 3 to immobilize MeHg.

The relationship between TOC and MeHg during day 20–80 was likely caused by the remaining organic matter existing in OSP. It has been observed that organic matter content seemed to play a critical role for MeHg formation, acting as electron donor for Hg methylation bacteria [42,43]. The sediment in Column 4 with more OSP would likely release a greater amount of MeHg. Without capping, TOC was possibly easier to release from sediment, which then caused the uprush of MeHg in Column 6 from day 85.

5. Conclusions

Based on the results obtained from the aqueous batch experiments, OSP and HAP had the optimum removal efficiencies to Cr, Zn, Cu, and Ni with CB taking the third place. As for Hg, FeS and CB showed the best immobilizing ability. Kaolinite presented the weakest removal performance towards all of these five metals, and lack of the presence of kaolinite did not show significant influence on the hydraulic stability of mixed caps.

Based on the lab-scale microcosm experiments, the mixing ratio of 10% kaolinite + 2.5% FeS + 2.5% CB + 35% HAP + 50% OSP (i.e., Column 5) had the most prominent effect to immobilize the five metals present in the test sediment. Although Column 4 (the lowest cost one) with 80% OSP showed unsuccessful results for reducing Ni and MeHg, it performed well in inhibiting the release of the other metals. When considering cost effectiveness and environmental impact, using caps mainly composed of OSP can yet be a good choice. But when applied to real sites, decisions should be made after comprehensive evaluations based on actual conditions.

This study helps to construct guidelines of using mixed materials mostly prepared from recycled materials to remediate multi-contaminated sediments and provide some references for active capping application and development. Results from this study would also be helpful in reducing the human health and ecological risks by reducing the potential toxic metal release from sediment to overlying water.

Supplementary Materials: The following are available online at <http://www.mdpi.com/2073-4441/12/7/1886/s1>, Figure S1: title, Table S1: Oxidation reduction potential (ORP) during operation, Table S2: pH values of microcosm during operation, Table S3: Dissolved oxygen (DO) (mg L⁻¹) of the overlying water in the microcosm, Table S4: Electrical conductivity (EC) of the overlying water in the microcosm, Table S5: THg concentration of the overlying water in the microcosm, Table S6: MeHg concentration of the overlying water in the microcosm, Table S7: Ni concentration of the overlying water in the microcosm, Table S8: Cr concentration of the overlying water in the microcosm, Table S9: Cu concentration of the overlying water in the microcosm, Table S10: Zn concentration of the overlying water in the microcosm.

Author Contributions: Conceptualization, M.-Y.O., Y.T., T.-C.C., and H.-C.H.; methodology, M.-Y.O., Y.T., B.-L.C., and C.C.; formal analysis, M.-Y.O., Y.T., B.-L.C., and Y.-H.C.; investigation, M.-Y.O.; data curation, M.-Y.O. and Y.-H.C.; writing—original draft preparation, M.-Y.O.; writing—review and editing, T.-C.C. and H.-C.H.; visualization, M.-Y.O.; funding acquisition, H.-C.H. All authors have read and agreed to the published version of the manuscript.

Funding: This project was financially supported by the Taiwan Environmental Protection Administration (No. 08BT547001).

Acknowledgments: We are very grateful to all members of the project team and the Groundwater Pollution Remediation Funds of Taiwan Environmental Protection Administration for their funding support.

Conflicts of Interest: The authors declare no conflict of interest.

References

1. Bouhamed, F.; Elouear, Z.; Bouzid, J.; Ouddane, B. Multi-component adsorption of copper, nickel and zinc from aqueous solutions onto activated carbon prepared from date stones. *Environ. Sci. Pollut. Res.* **2016**, *23*, 15801–15806. [[CrossRef](#)]
2. Kutuniva, J.; Mäkinen, J.; Kauppila, T.; Karppinen, A.; Hellsten, S.; Luukkonen, T.; Lassi, U. Geopolymers as active capping materials for in situ remediation of metal (loid)-contaminated lake sediments. *J. Environ. Chem. Eng.* **2019**, *7*, 102852. [[CrossRef](#)]
3. Zhang, C.; Zhu, M.Y.; Zeng, G.M.; Yu, Z.G.; Cui, F.; Yang, Z.Z.; Shen, L.Q. Active capping technology: A new environmental remediation of contaminated sediment. *Environ. Sci. Pollut. Res.* **2016**, *23*, 4370–4386. [[CrossRef](#)] [[PubMed](#)]
4. Race, M.; Nabelkova, J.; Fabbricino, M.; Pirozzi, F.; Raia, P. Analysis of heavy metal sources for urban creeks in the Czech Republic. *Water Air Soil Pollut.* **2015**, *226*, 322. [[CrossRef](#)]
5. Salomons, W.; De Rooij, N.M.; Kerdiijk, H.; Bril, J. Sediments as a source for contaminants? *Hydrobiologia* **1987**, *149*, 13–30. [[CrossRef](#)]

6. Zoumis, T.; Schmidt, A.; Grigorova, L.; Calmano, W. Contaminants in sediments: Remobilisation and demobilisation. *Sci. Total Environ.* **2001**, *266*, 195–202. [[CrossRef](#)]
7. Hsu, T.C. Experimental assessment of adsorption of Cu^{2+} and Ni^{2+} from aqueous solution by oyster shell powder. *J. Hazard. Mater.* **2009**, *171*, 995–1000. [[CrossRef](#)]
8. Jiang, M.Q.; Jin, X.Y.; Lu, X.Q.; Chen, Z.L. Adsorption of Pb (II), Cd (II), Ni (II) and Cu (II) onto natural kaolinite clay. *Desalination* **2010**, *252*, 33–39. [[CrossRef](#)]
9. Latifi, Z.; Jalali, M. Measuring and simulating Co (II) sorption on waste calcite, zeolite and kaolinite. *Nat. Resour. Res.* **2019**, 1–15. [[CrossRef](#)]
10. Jalees, M.I.; Farooq, M.U.; Basheer, S.; Asghar, S. Removal of Heavy Metals from Drinking Water Using Chikni Mitti (Kaolinite): Isotherm and Kinetics. *Arabian J. Sci. Eng.* **2019**, *44*, 6351–6359. [[CrossRef](#)]
11. Alasadi, A.; Khaili, F.; Awwad, A. Adsorption of Cu (II), Ni (II) and Zn (II) ions by nano kaolinite: Thermodynamics and kinetics studies. *Chem. Int.* **2019**, *5*, 258–268.
12. Jeong, H.Y.; Klaue, B.; Blum, J.D.; Hayes, K.F. Sorption of mercuric ion by synthetic nanocrystalline mackinawite (FeS). *Environ. Sci. Technol.* **2007**, *44*, 7699–7705. [[CrossRef](#)] [[PubMed](#)]
13. Xiong, Z.; He, F.; Zhao, D.; Barnett, M.O. Immobilization of mercury in sediment using stabilized iron sulfide nanoparticles. *Water Res.* **2009**, *43*, 5171–5179. [[CrossRef](#)] [[PubMed](#)]
14. Feng, Y.; Gong, J.L.; Zeng, G.M.; Niu, Q.Y.; Zhang, H.Y.; Niu, C.G.; Yan, M.; Deng, J.-H. Adsorption of Cd (II) and Zn (II) from aqueous solutions using magnetic hydroxyapatite nanoparticles as adsorbents. *Chem. Eng. J.* **2010**, *162*, 487–494. [[CrossRef](#)]
15. Jang, S.H.; Min, B.G.; Jeong, Y.G.; Lyoo, W.S.; Lee, S.C. Removal of lead ions in aqueous solution by hydroxyapatite/polyurethane composite foams. *J. Hazard. Mater.* **2008**, *152*, 1285–1292. [[CrossRef](#)]
16. Krestou, A.; Xenidis, A.; Panias, D. Mechanism of aqueous uranium (VI) uptake by hydroxyapatite. *Miner. Eng.* **2004**, *17*, 373–381. [[CrossRef](#)]
17. Narwade, V.N.; Khairnar, R.S.; Kokol, V. In situ synthesized hydroxyapatite—Cellulose nanofibrils as biosorbents for heavy metal ions removal. *J. Polym. Environ.* **2018**, *26*, 2130–2141. [[CrossRef](#)]
18. Kumar, G.S.; Girija, E.K.; Venkatesh, M.; Karunakaran, G.; Kolesnikov, E.; Kuznetsov, D. One step method to synthesize flower-like hydroxyapatite architecture using mussel shell bio-waste as a calcium source. *Ceram. Int.* **2017**, *43*, 3457–3461. [[CrossRef](#)]
19. Wu, Q.; Chen, J.; Clark, M.; Yu, Y. Adsorption of copper to different biogenic oyster shell structures. *Appl. Surf. Sci.* **2014**, *311*, 264–272. [[CrossRef](#)]
20. Moon, D.H.; Wazne, M.; Cheong, K.H.; Chang, Y.Y.; Baek, K.; Ok, Y.S.; Park, J.H. Stabilization of As-, Pb-, and Cu-contaminated soil using calcined oyster shells and steel slag. *Environ. Sci. Pollut. Res.* **2015**, *22*, 11162–11169. [[CrossRef](#)]
21. Ahmad, M.; Lee, S.S.; Yang, J.E.; Ro, H.M.; Lee, Y.H.; Ok, Y.S. Effects of soil dilution and amendments (mussel shell, cow bone, and biochar) on Pb availability and phytotoxicity in military shooting range soil. *Ecotoxicol. Environ. Saf.* **2012**, *79*, 225–231. [[CrossRef](#)] [[PubMed](#)]
22. Ahmad, M.; Lee, S.S.; Lim, J.E.; Lee, S.E.; Cho, J.S.; Moon, D.H.; Hashimoto, Y.; Ok, Y.S. Speciation and phytoavailability of lead and antimony in a small arms range soil amended with mussel shell, cow bone and biochar: EXAFS spectroscopy and chemical extractions. *Chemosphere.* **2014**, *95*, 433–441. [[CrossRef](#)] [[PubMed](#)]
23. EPA Taiwan. *Investigation of Sediment Pollution Sources and Transmission Mode-Taking Key Rivers as Examples*; Taiwan Environmental Protection Administration: Taipei, Taiwan, 2011; EPA-100-GA102-02-A232.
24. ASTM D2765-16. *Standard Test Methods for Determination of Gel Content and Swell Ratio of Crosslinked Ethylene Plastics*; ASTM International: West Conshohocken, PA, USA, 2016; Available online: www.astm.org (accessed on 1 July 2020).
25. Wu, S.C.; Tsou, H.K.; Hsu, H.C.; Hsu, S.K.; Liou, S.P.; Ho, W.F. A hydrothermal synthesis of eggshell and fruit waste extract to produce nanosized hydroxyapatite. *Ceram. Int.* **2013**, *39*, 8183–8188. [[CrossRef](#)]
26. Trinkunaite-Felsen, J.; Prichodko, A.; Semasko, M.; Skaudzius, R.; Beganskiene, A.; Kareiva, A. Synthesis and characterization of iron-doped/substituted calcium hydroxyapatite from seashells *Macoma balthica* (L.). *Adv. Powder Technol.* **2015**, *26*, 1287–1293. [[CrossRef](#)]
27. Sobczak-Kupiec, A.; Malina, D.; Kijkowska, R.; Wzorek, Z. Comparative study of hydroxyapatite prepared by the authors with selected commercially available ceramics. *Digest J. Nanomater. Biostructures* **2012**, *7*, 385–391.

28. Lewis, P.A. *Short-Term Methods for Estimating the Chronic Toxicity of Effluents and Receiving Waters to Freshwater Organisms*; EPA, Environmental Monitoring Systems Laboratory: Cincinnati, OH, USA, 1994.
29. Ting, Y.; Chen, C.; Ch'ng, B.L.; Wang, Y.L.; Hsi, H.C. Using raw and sulfur-impregnated activated carbon as active cap for leaching inhibition of mercury and methylmercury from contaminated sediment. *J. Hazard. Mater.* **2018**, *354*, 116–124. [[CrossRef](#)]
30. Ting, Y.; Ch'ng, B.L.; Chen, C.; Ou, M.Y.; Cheng, Y.H.; Hsu, C.J.; Hsi, H.C. A simulation study of mercury immobilization in estuary sediment microcosm by activated carbon/clay-based thin-layer capping under artificial flow and turbation. *Sci. Total Environ.* **2020**, *708*, 135068. [[CrossRef](#)]
31. Kwapinski, W.; Byrne, C.M.; Kryachko, E.; Wolfram, P.; Adley, C.; Leahy, J.J.; Hayes, M.H.; Novotny, E. Biochar from biomass and waste. *Waste Biomass Valoriz.* **2010**, *1*, 177–189. [[CrossRef](#)]
32. Kay, M.I.; Young, R.A.; Posner, A.S. Crystal structure of hydroxyapatite. *Nature* **1964**, *204*, 1050–1052. [[CrossRef](#)]
33. Wang, X.; Yu, R.; Wang, P.; Chen, F.; Yu, H. Co-modification of F⁻ and Fe (III) ions as a facile strategy towards effective separation of photogenerated electrons and holes. *Appl. Surf. Sci.* **2015**, *351*, 66–73. [[CrossRef](#)]
34. Fuller, C.C.; Bargar, J.R.; Davis, J.A.; Piana, M.J. Mechanisms of uranium interactions with hydroxyapatite: Implications for groundwater remediation. *Environ. Sci. Technol.* **2002**, *36*, 158–165. [[CrossRef](#)] [[PubMed](#)]
35. Lee, C.H.; Lee, D.K.; Ali, M.A.; Kim, P.J. Effects of oyster shell on soil chemical and biological properties and cabbage productivity as a liming materials. *Waste Manag.* **2008**, *28*, 2702–2708. [[CrossRef](#)] [[PubMed](#)]
36. Glatstein, D.A.; Francisca, F.M. Influence of pH and ionic strength on Cd, Cu and Pb removal from water by adsorption in Na-bentonite. *Appl. Clay Sci.* **2015**, *118*, 61–67. [[CrossRef](#)]
37. Singh, S.P.; Ma, L.Q.; Tack, F.M.; Verloo, M.G. Trace metal leachability of land-Disposed dredged sediments. *J. Environ. Qual.* **2000**, *29*, 1124–1132. [[CrossRef](#)]
38. Li, H.; Shi, A.; Li, M.; Zhang, X. Effect of pH, temperature, dissolved oxygen, and flow rate of overlying water on heavy metals release from storm sewer sediments. *J. Chem.* **2013**, 434012. [[CrossRef](#)]
39. Zhai, X.; Li, Z.; Huang, B.; Luo, N.; Huang, M.; Zhang, Q.; Zeng, G. Remediation of multiple heavy metal-contaminated soil through the combination of soil washing and in situ immobilization. *Sci. Total Environ.* **2018**, *635*, 92–99. [[CrossRef](#)]
40. Calmano, W.; Hong, J.; Förstner, U. Binding and mobilization of heavy metals in contaminated sediments affected by pH and redox potential. *Water Sci. Technol.* **1993**, *28*, 223–235. [[CrossRef](#)]
41. Mehrotra, A.S.; Horne, A.J.; Sedlak, D.L. Reduction of net mercury methylation by iron in *Desulfobulbus propionicus* (1pr3) cultures: Implications for engineered wetlands. *Environ. Sci. Technol.* **2003**, *37*, 3018–3023. [[CrossRef](#)]
42. Parks, J.M.; Johs, A.; Podar, M.; Bridou, R.; Hurt, R.A.; Smith, S.D.; Brandt, C.C.; Palumbo, A.V. The genetic basis for bacterial mercury methylation. *Science* **2013**, *339*, 1332–1335. [[CrossRef](#)]
43. Bravo, A.G.; Bouchet, S.; Tolu, J.; Björn, E.; Mateos-Rivera, A.; Bertilsson, S. Molecular composition of organic matter controls methylmercury formation in boreal lakes. *Nat. Commun.* **2017**, *8*, 1–9. [[CrossRef](#)]

